Maximizing the peak lift-to-drag coefficient ratio of airfoils by optimizing the ratio of thickness to the camber of airfoils

Hossein Seifi Davari[*a] , Mohsen Seify Davari[b], Ruxandra Mihaela Botez[c], Harun Chowdhury[d]

[a] Department of Mechanical & Marine Engineering, Chabahar Maritime University, Chabahar, Iran
[b] Faculty of Engineering and Technology, Islamic Azad University, Germi, Iran
[c] Laboratory of Applied Research in Active Controls, Avionics, and AeroServoElasticity LARCASE, ÉTS-École de Technologie Supérieure, Université de Québec, Montréal, QC H3C 1K3, Canada
[d] School of Engineering, RMIT University, Melbourne, VIC-3000, Australia

A B S T R A C T

The paper investigates the lift-to-drag coefficient ratio (CL/CD) efficiency of three airfoils, namely E387, RG15, and SD6060. The objective is to optimize the airfoils for maximum CL/CD efficiency and evaluate them using XFOIL software. The study focuses on these airfoils' performance at different Reynolds numbers (Re) from 500,000 to 1,000,000, with varying thickness-to-camber ratio percentages (t/c%). The results indicate that the E387-Opt airfoil improved the maximum CL/CD by 18.92% at Re 500,000, 23.77% at Re 600,000, 27.14% at Re 700,000, 32.44% at Re 800,000, 32.93% at Re 900,000, and 38.46% at Re 1,000,000. The RG15-Opt airfoil also demonstrated impressive performance, with a maximum CL/CD increase of 34.38% at Re 500,000, 36.75% at Re 600,000, 38.54% at Re 700,000, 41.58% at Re 800,000, 45.57% at Re 900,000, and 51.30% at Re 1,000,000. Finally, the SD6060-Opt airfoil showed even better results, with a maximum CL/CD increase of 37.07% at Re 500,000, 38.16% at Re 600,000, 42.44% at Re 700,000, 48.99% at Re 800,000, 53.10% at Re 900,000, and 56.91% at Re 1,000,000.

A R T I C L E   I N F O

1. Introduction

Wind power is a crucial source of clean and affordable green energy (Seifi et al., 2023). The design of airfoil geometry is crucial to achieving optimal aerodynamic efficiency, leading to extensive research into developing dedicated airfoil geometries based on specific design conditions (Tirandaz and Rezaeiha, 2021). Improved lift coefficients (CL) with angle of attack (AoA) have been achieved through the use of new slot designs (Bhavsar et al., 2023; Jaffar et al., 2023; Mohamed et al., 2020), serrated Gurney flaps (Ye et al., 2023), double vortex generators (Özden et al., 2023), vibrating cylinders (Chen et al., 2023), flaps mounted with torsional springs (Flynn and Goza, 2023), and optimized jets (Kasmaiee et al., 2023). However, the presence of a dent can negatively impact the efficiency of airfoils, causing a decrease in CL and an increase in CD (Wani et al., 2023). Flow control accessories on bionic airfoils have improved their static CL (Wu et al., 2022). The leading-edge protuberances method has also demonstrated the potential to maintain high aerodynamic efficiency (Zhang et al., 2021), while the laminar separation method has effectively restrained the phenomenon, resulting in improved CL and decreased CD (Lei et al., 2020).

Static micro-cylinders have also been shown to efficiently suppress flow separation and enhance the aerodynamic efficiency of airfoils (Shi et al., 2019). Finally, XFOIL software has been demonstrated to effectively predict wind tunnel results at low Re (Seifi Davari et al., 2023). Numerous studies have been conducted to improve the performance of airfoils. These studies have explored various methods such as slot design, serrated Gurney flap, double vortex generator, single vibrating cylinder, leading-edge protuberances, laminar separation, and the static micro-cylinder methods. This paper uses the CL/CD efficiency of the E387, RG15, and SD6060 airfoils at different t/c% as a basis for optimizing modified airfoils. The results show that as the Reynolds number increases from 500,000 to 1,000,000, the maximum CL/CD decreases. Subsequently, the airfoils are modified and evaluated using XFOIL software.

This study compares the E387, RG15, and SD6060 airfoils with the modified airfoils using the XFOIL software and a Reynolds number of 500,000 to 1,000,000.

2. Material and Methods

2.1. Investigating the peak CL/CD of airfoils

Figs. 1, 2 and 3 show the maximum CL/CD for three airfoils – E387, RG15, and SD6060. Fig. 1 demonstrates that the E387 airfoil achieved its highest maximum CL/CD ratio at a Reynolds number (Re) of 900,000, reaching 116.70 at an angle of attack (AoA) of 3º. The lowest maximum CL/CD was recorded at a Re of 500,000, 105.80 at an AoA of 4º. The maximum CL/CD values of 116.40, 113.30, 112.60, and 109.20 were recorded at Re of 1,000,000, 800,000, 700,000, and 600,000 respectively.
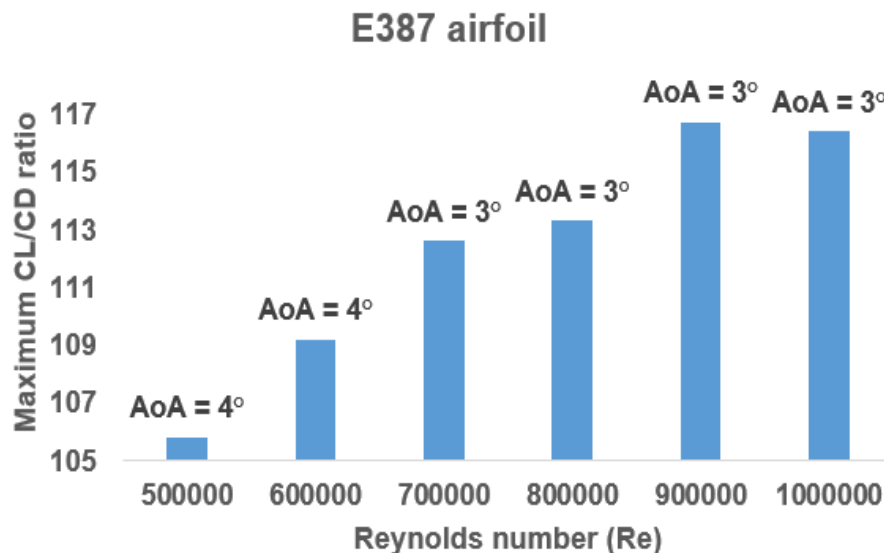

Fig. 1. The peak CL/CD with the AoA variation of the E387 airfoil.

Based on the data presented in Fig. 2, it can be observed that the RG15 airfoil performs best in terms of maximum CL/CD value at a Reynolds number (Re) of 900,000. At this Re, the highest maximum CL/CD value was recorded at 96.43 at an angle of attack (AoA) of 3º. On the other hand, the lowest maximum CL/CD value was recorded at Re of 500,000, which was 77.50 at an AoA of 4º. Other maximum CL/CD values recorded were 96.20, 95.44, 94.85, and 92.92 at Re of 800,000, 700,000, 1,000,000, and 600,000, respectively.

According to the findings presented in Fig. 3, the SD6060 airfoil showed the highest maximum CL/CD at a Re of 700,000, which was 98.33 at an AoA of 4º. On the other hand, the lowest maximum CL/CD was recorded at a Re of 500,000, which was 93.30 at an AoA of 4º. The maximum CL/CD values of 97.70, 97.60, 97.30 and 97.25 were achieved at Re of 600,000, 800,000, 900,000, and 1,000,000, respectively.
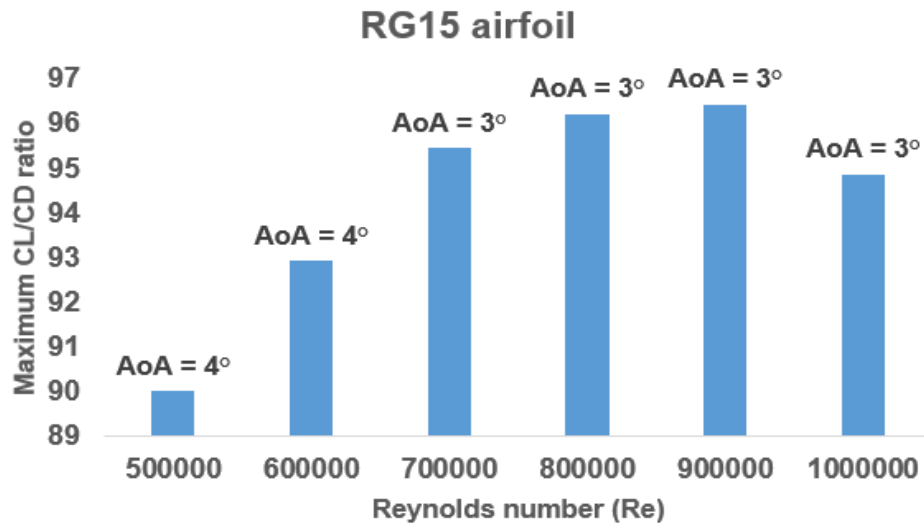
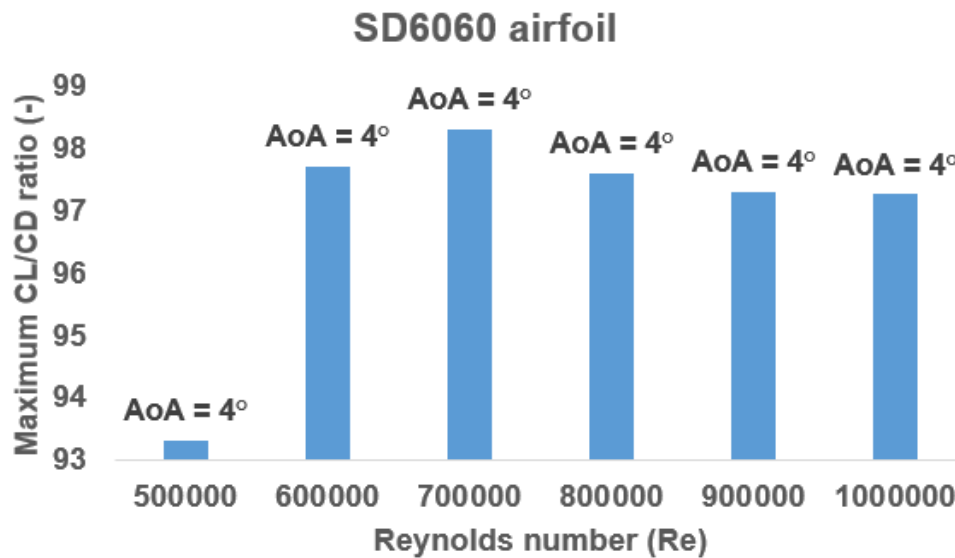**Fig. 2.** The peak CL/CD variation with the AoA of the RG15 airfoil.

Fig. 3. The peak CL/CD variation with the AoA of the SD6060 airfoil.

2.2. Airfoil selection

XFOIL software, developed by Dr. Mark Drela at MIT, uses a sophisticated mathematical model to analyze airfoils. It combines viscous and inviscid interactions and uses a unique linear-vorticity panel method with Karman-Tsien compressibility correction. To model viscous layer effects on potential flow outcomes, XFOIL can perform versatile analyses in direct and mixed-inverse modes, including the overlay of source distributions on airfoils and wakes. Its two-equation lagged dissipation integral method accommodates laminar and turbulent flows. In contrast, the global Newton method concurrently solves boundary layer and transition equations with the inviscid flow field. XFOIL's computational

backbone is tailored for subcritical airfoil design and is particularly effective at low Reynolds numbers (Re). Its graphic-oriented routines make it easy for designers to analyze, invert, and modify geometries with an intuitive menu structure, offering unprecedented flexibility. XFOIL ensures that modifications are grounded in physical principles, empowering designers to explore novel approaches and tailor designs to specific needs. XFOIL's capabilities extend beyond airfoil design, encompassing inverse design, dynamic coordinate mixing, boundary layer computation, general analysis, and parametric design. Anastasiia's (2022) study further supports XFOIL's efficacy in crafting subcritical airfoils, especially at low Re. Its visually oriented procedures provide extensive

flexibility for analyses, inversions, and alterations, enhancing its applicability across various design domains. The RG15, E387, and SD6060 airfoils were selected as baseline models for airfoil optimization due to their well-

established aerodynamic efficiency at low Re. Fig. 4 showcases their geometric features and highlights the various components of a typical airfoil.
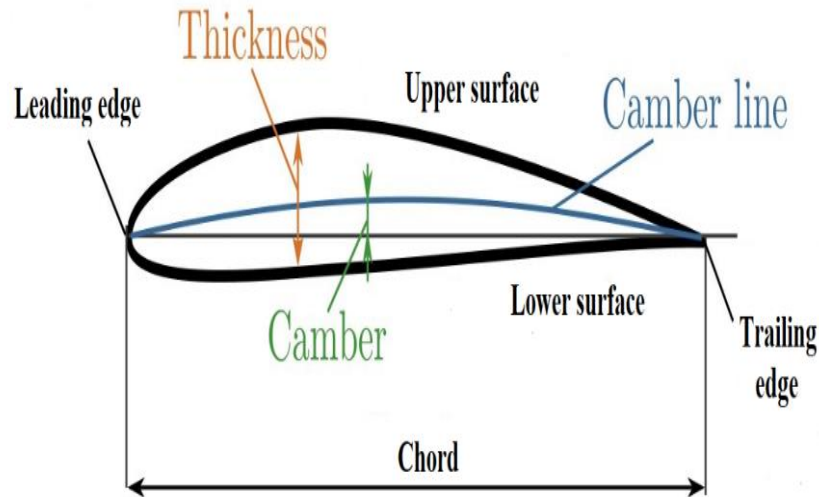

Fig. 4. Schematic diagram of the airfoil.

The airfoils RG15, E387, and SD6060 were chosen as baseline airfoils for the present study because of their excellent aerodynamic performance in low Reynolds number situations. XFOIL software was used to modify the geometry of the base airfoils, resulting in the creation of novel airfoils by adjusting their thicknesses and camber settings. These new airfoils' peak CL/CD was analyzed at Reynolds numbers of 500,000 to 1,000,000 for various t/c% configurations. The t/c% zone that exhibited the highest CL/CD was then used to calculate the geometrical parameters of the modified airfoils, enabling the evaluation of their optimal aerodynamic performance. Fig. 5 illustrates the algorithm for identifying the optimal modified airfoil geometries tested in XFOIL software. Viscous airflow investigations were conducted at Reynolds numbers of 500,000 to 1,000,000 and AoAs ranging from 0° to 20°. The performance parameters for the three innovative airfoils that were developed and modified are presented in the following section.

2.3. XFOIL flowchart

The algorithm used to determine the geometries of the optimized airfoils is depicted in Fig. 5. XFOIL software analyses the airfoils through viscous airflow simulations within a Re range of 500,000 to 1,000,000 and AoA variations

from 0° to 20°. Here is a detailed explanation of the flowchart:
Step 1: Baseline airfoil selection
Initially, three baseline airfoils are chosen for further optimization to enhance their aerodynamic efficiency.
Step 2: Airfoil optimization using t/c%
The selected baseline airfoils undergo iterative modifications based on changes in the t/c% (thickness-to-chord ratio). Different t/c% values are investigated to develop innovative airfoil designs, each customized to meet specific aerodynamic performance criteria, focusing on CL/CD (lift-to-drag ratio).
Step 3: Optimized airfoil development
Novel airfoil designs are crafted by adjusting the t/c% across a range of values, generating a spectrum of designs suitable for Re ranging from 500,000 to 1,000,000.
Step 4: Comparative analysis
A thorough comparative analysis is conducted to evaluate the aerodynamic efficiency of the developed airfoils compared to the baseline models. The key aerodynamic parameter, CL/CD, is scrutinized.
Step 5: Aerodynamic performance and optimized airfoil selection
Optimized airfoils demonstrating superior aerodynamic performance, with maximum CL/CD compared to the baseline airfoils, are selected for further scrutiny.
Step 6: Iterative refinement

Airfoils exhibiting lower efficiency metrics than the baseline models undergo additional rounds of optimization, focusing on fine-tuning the t/c% to enhance their aerodynamic performance further.

Step 7: Iterative assessment
The iterative process of optimization, analysis, and comparison persists as the airfoils undergo successive evaluations at different t/c% and Re values. This iterative approach aims to determine the optimal t/c% for each airfoil, continuously striving for improved aerodynamic performance. This systematic and iterative approach within the XFOIL software allows for thorough assessment and optimization of airfoils, focusing on their t/c% values. This leads to identifying optimized designs specifically tailored to enhance aerodynamic efficiency within Small Wind Turbine (SWT) technology.
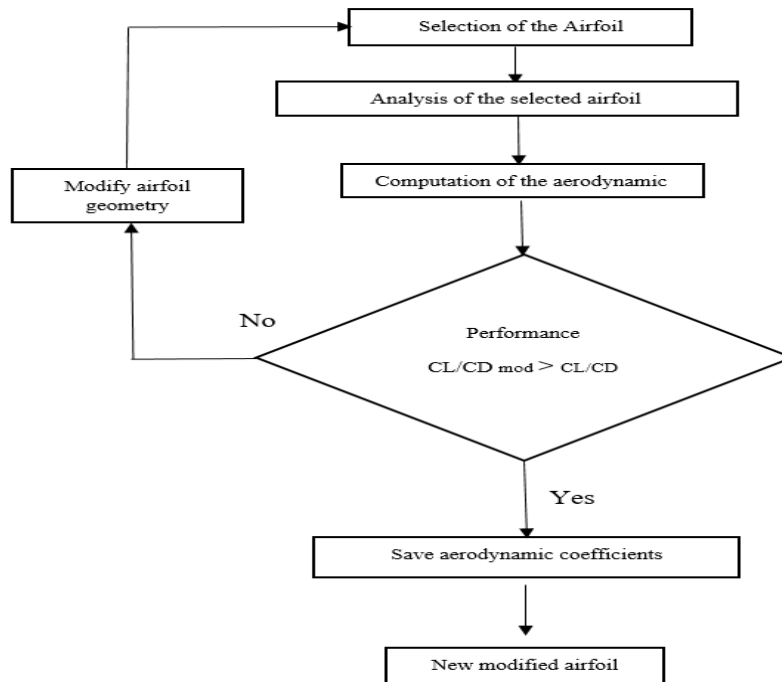
Fig. 5. Abstract of XFOIL software process for airfoil analysis.

2.4. Theoretical framework

The theoretical basis for investigating the aerodynamic characteristics of the airfoils is provided by Eqs. (1) to (3) (Manwell et al., 2009). The Re is defined by:

$$Re = \frac{U\,L}{v} = \frac{\rho\,U\,L}{\mu} = \frac{Inertial\ force}{Viscous\ force} \quad (1)$$

Where ρ is the fluid density, μ is the fluid viscosity. $v = \mu/\rho$ is the kinematic viscosity, and U and L are values of speed and length that characterize the air. These values could be the incoming wind speed, U_{wind}, and the chord length of an airfoil. The two-dimensional CL is defined as (Seifi et al., 2023):

$$CL = \frac{L/l}{\frac{1}{2}\rho U^2 c} = \frac{Lift\ force/unit\ length}{Dynamic\ force/unit\ length} \quad (2)$$

The two-dimensional CD is obtained as:

$$CD = \frac{D/l}{\frac{1}{2}\rho U^2 c} = \frac{Drag\ force/unit\ length}{Dynamic\ force/unit\ length} \quad (3)$$

Where c is the airfoil chord length, l is the airfoil span, L is the lift force, and D is the drag force.

2.5. Airfoil optimization

2.5.1. The E387 Airfoil Optimization
The efficiency of the airfoil identified as E387 was used as the basis for modified airfoil optimization, considering various thickness-to-chord ratios. Table 1 provides details of the thicknesses, cambers, and the ratios of t/c% that were analyzed. At the same time, Fig. 6 illustrates the highest variation in the lift-to-drag ratio with t/c% at Reynolds numbers ranging from 500,000 to 1,000,000 for the E387 airfoil. As per Fig. 6, the highest lift-to-drag ratio is observed in the t/c% range of 0.50% to 1.31% for Reynolds numbers between 500,000 and 1,000,000. Any further increase in t/c% results in a decrease in the aerodynamic performance of the airfoil. Therefore, the optimal range of t/c% considered while developing the E387 airfoil was between 0.50% and 1.31%.

Table 1. An investigation of the thicknesses and cambers for the E387 airfoil

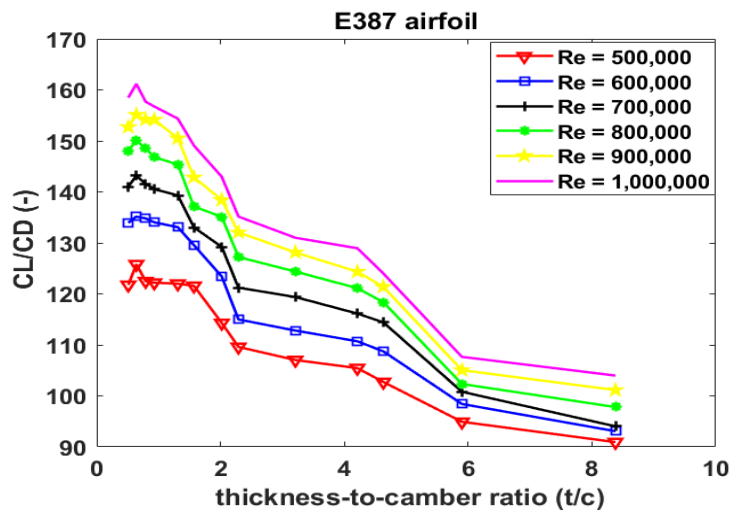| t/c%	t%	at (%)	c%	at (%)
0.51%	3.46	12.90	6.77	36.5
0.64%	4.15	30.6	6.40	37.80
0.79%	4.79	27.70	6.00	40.60
0.93%	5.36	30.50	5.73	40.50
1.31%	6.62	32.70	5.03	38.00
1.57%	7.54	32.40	4.78	39.80
2.02%	8.47	31.60	4.18	40.20
2.29%	9.15	29.82	3.98	41.90
2.38% (E387 airfoil)	9.07	31.13	3.80	40.13
3.21%	10.53	30.50	3.28	38.20
4.21%	11.21	33.60	2.66	39.20
4.63%	11.69	30.40	2.52	38.50
5.90%	12.08	35.00	2.05	35.00
8.38%	13.42	35.70	1.60	38.10

Fig. 6. The maximum CL/CD performance of airfoils with various t/c% for the E387 airfoil in the range Re = 500,000 to 1,000,000.

The E387 airfoil developed with a t/c% of 0.64% is called the E387-Opt airfoil, optimized to have a pick thickness of 4.15% at 30.60% of the chord, and a pick camber of 6.40% at 37.80% of the chord. The E387 airfoil has a pick thickness of 9.07% at 31.13% of the chord and a pick camber of 3.80% at 40.13%. Fig 7 illustrates the E387 and the E387-Opt airfoils at Re of 500,000 to 1,000,000.
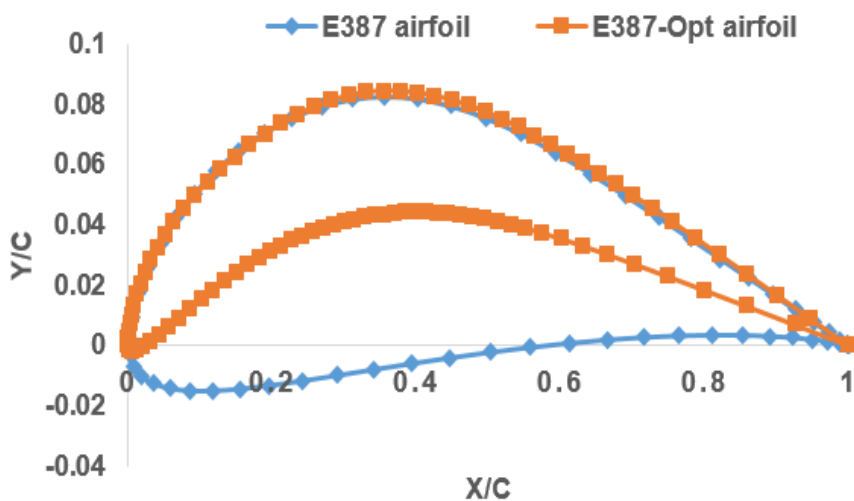

Fig. 7. Airfoil shape variation for E387 airfoil optimization at Re of 500,000 to 1,000,000.

2.5.2. The RG15 Airfoil Optimization

The CL/CD efficiency of the RG15 airfoil with various t/c% was used here as the basis for the modified airfoil optimization. Table 2 lists the thicknesses and cambers and the ratios of the t/c% analyzed here, while Fig. 8 illustrates the highest CL/CD variation with t/c% at Re of

500,000 to 1,000,000 for the RG15 airfoil. According to Fig. 8, for Re of 500,000 to 1,000,000, the peak CL/CD occurs in the t/c% ranges from 0.51% to 1.00%; the aerodynamic

performance of the airfoil decreases with any further increase in the t/c%. Hence, the t/c% considered when developing the RG15 airfoil was between 0.51% and 1.00%.

Table 2. An investigation of the thicknesses and cambers for the RG15 airfoil

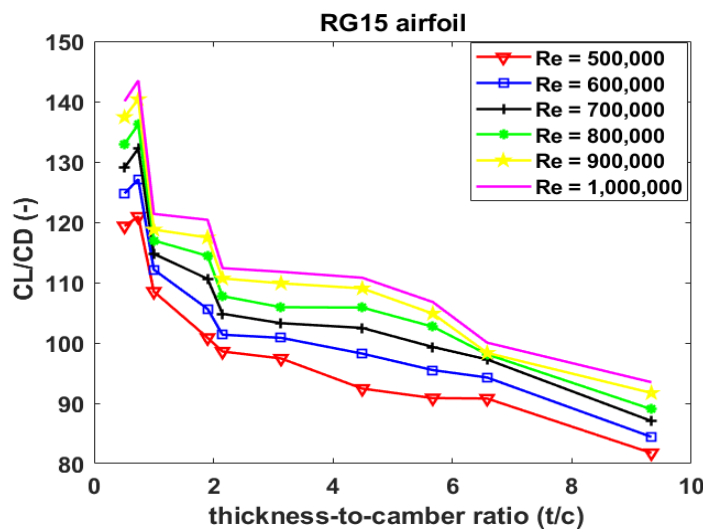| t/c%	t%	at (%)	c%	at (%)
0.51%	2.59	29.50	4.99	36.80
0.74%	3.43	21.70	4.61	41.00
1.00%	3.62	18.10	3.62	36.50
1.90%	6.22	27.00	3.27	34.90
2.15%	6.39	36.20	2.97	37.30
3.13%	7.81	29.90	2.49	42.50
4.49%	8.86	35.00	1.97	32.20
5.06% (RG15 airfoil)	8.92	30.30	1.76	39.70
5.67%	9.53	30.30	1.68	39.80
6.58%	9.87	35.60	1.50	47.20
9.33%	12.23	31.30	1.31	61.10

Fig. 8. The maximum CL/CD performance of airfoils with various t/c% for the RG15 airfoil in the range Re = 500,000 to 1,000,000.

The RG15 airfoil, developed with a thickness-to-chord ratio of 0.74%, has been optimized to create the RG15-Opt airfoil. The new airfoil has a peak thickness of 3.43% located at 21.70% of the chord, and a peak camber of 4.61% at 41% of the chord. The original RG15 airfoil has a

peak thickness of 8.92% at 30.30% of the chord and a peak camber of 1.76% at 39.70%. Fig. 9 illustrates the RG15 and RG15-Opt airfoils at Reynolds numbers ranging from 500,000 to 1,000,000.
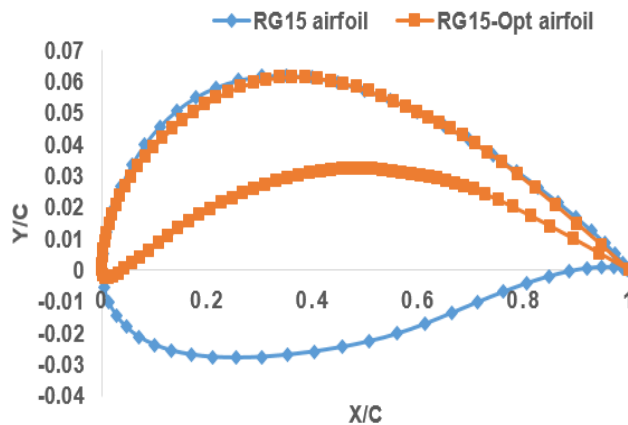

Fig. 9. Airfoil shape variation for RG15 airfoil optimization at Re of 500,000 to 1,000,000.

2.5.3. The SD6060 Airfoil Optimization

The efficiency of the CL/CD of the airfoil with plate number 1 was used as the basis for the modified airfoil optimization, which analyzed various t/c% ratios. Table 3 lists the thicknesses and cambers of the airfoil, while Fig. 10 shows the highest CL/CD variation with t/c% at a Reynolds number of 500,000 to 1,000,000.

According to Fig. 10, the peak CL/CD of the airfoil occurs in the t/c% range of 0.40% to 1.00% for Reynolds numbers of 500,000 to 1,000,000. The aerodynamic performance of the airfoil decreases as the t/c% increases beyond this range. Therefore, the t/c% considered when developing the airfoil with plate number 1 was between 0.40% and 1.00%.

Table 3. An investigation of the thicknesses and cambers for the SD6060 airfoil

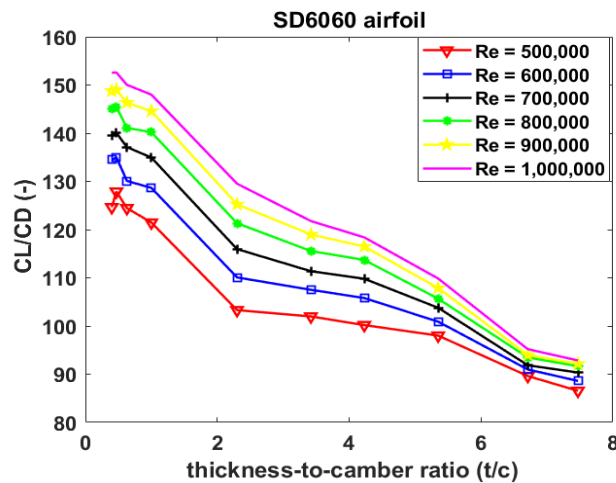| t/c%	t%	at (%)	c%	at (%)
0.40%	2.39	25.00	5.96	32.90
0.47%	2.76	8.60	5.81	36.90
0.63%	3.42	16.00	5.40	37.20
1.00%				
	4.77	34.90	4.77	34.50
2.30%	7.73	31.70	3.36	36.90
3.42%	9.22	33.30	2.69	38.70
4.23%	9.90	31.20	2.34	39.40
5.35%	10.77	33.90	2.01	44.00
5.60% (SD6060 airfoil)	10.37	33.92	1.85	38.52
6.71%	10.81	31.50	1.61	38.50
7.47%	11.36	32.80	1.52	37.80

Fig. 10. The maximum CL/CD performance of airfoils with various t/c% for the SD6060 airfoil in the range Re = 500,000 to 1,000,000.

The SD6060 airfoil developed with a t/c% of 0.47% is called the SD6060-Opt airfoil. It is optimized to have a pick thickness of 2.76% at 8.60% of the chord and a pick camber of 5.81% at 36.90%. The SD6060 airfoil has a pick thickness of 10.37% at 33.92% of the chord and a pick camber of 1.85% at 38.52%. Fig. 11 illustrates the SD60 and the SD6060-Opt airfoils at Re of 500,000 to 1,000,000.
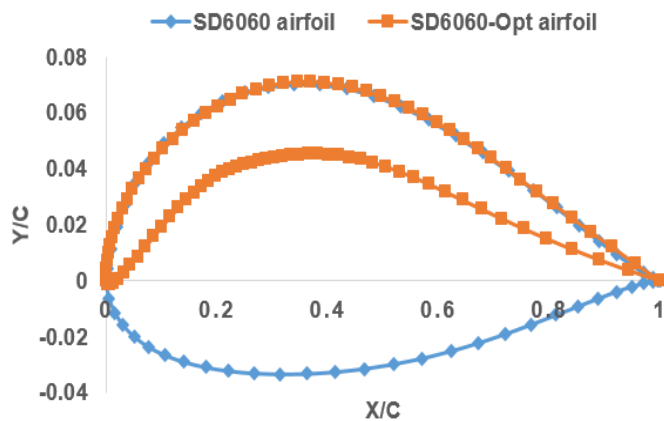

Fig. 11. Airfoil shape variation for SD6060 airfoil optimization at Re of 500,000 to 1,000,000.

3. Results and discussion

3.1. Validation data

To validate our current research, we analyzed the variation of the CL with the AoA and the CD with the AoA variation using XFOIL software. We then compared the results to wind tunnel data from the UIUC low-turbulence subsonic wind tunnel (Leloudas et al., 2020) and 2D RANS solver (Morgado et al., 2016). The variations of the CL with the AoA and CD with the AoA for the RG15 airfoil are presented in Figs. 12(a) and (b), respectively. It's worth noting that the Re of 300,000 corresponds to the lower and higher points of the Re spectrum studied during the experimental investigation.
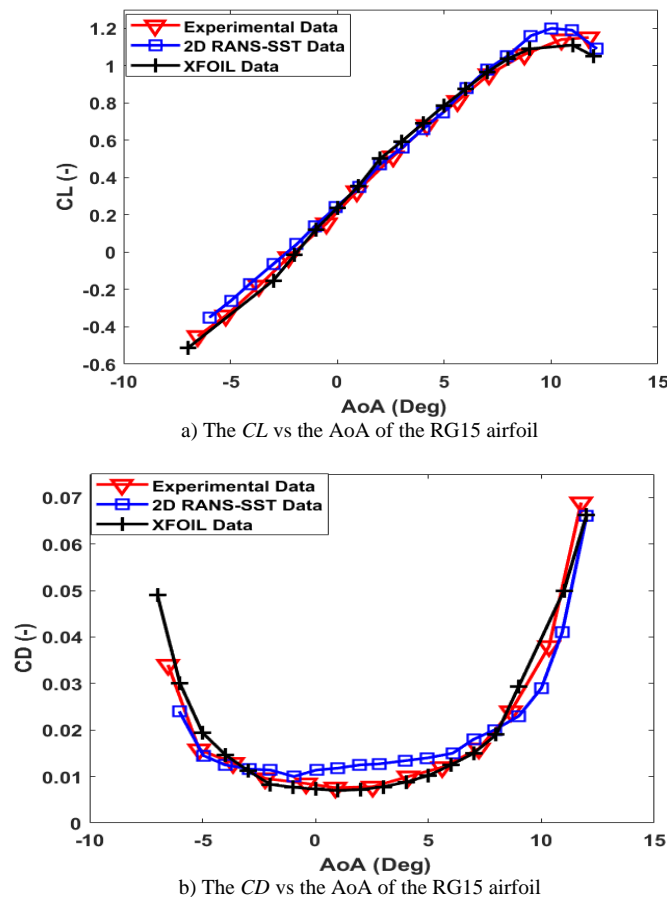

a) The *CL* vs the AoA of the RG15 airfoil

b) The *CD* vs the AoA of the RG15 airfoil

Fig. 12. Variation of aerodynamic parameters calculated utilizing XFOIL software compared to the wind tunnel data from the UIUC low-turbulence subsonic wind tunnel (Leloudas et al., 2020) and 2D RANS solver (Morgado et al., 2016) at a *Re* of 300,000 with for an RG15 airfoil: a) CL vs the AoA, b) CD vs the AoA.

The XFOIL software accurately predicted the same results as the others. On the one hand, an overestimation of CD was observed, particularly at AoAs ranging from -3° to 6°, a typical characteristic of the 2D RANS solver (Morgado et al., 2016).

3.2. Comparison of the CL/CD of reference airfoils with modified airfoils

3.2.1. Comparison of the CL/CD of Reference Airfoils with those of Altered Airfoils

Fig. 13 displays the CL/CD performance of the original and altered airfoils at a Re of 500,000. As per the data in Fig. 13, the E387-Opt airfoil outperforms the E387 base and other modified airfoils in CL/CD investigations, especially for an AoA ranging from 0° to 15°. The maximum CL/CD of 125.82 was recorded by the E387-Opt airfoil at an AoA of 5°, which is greater than the E387 airfoil's maximum CL/CD of 105.80 at an AoA of 4°. By adjusting the shape of the RG15 airfoil, the maximum CL/CD rose from 90 at an AoA of 4° to 120.95 at an AoA of 3°. The highest increase in maximum CL/CD was accomplished by modifying the SD6060 airfoil to SD6060-Opt, which resulted in an increase from 93.30 with the SD6060 to 127.89, with a similar AoA of 4°.
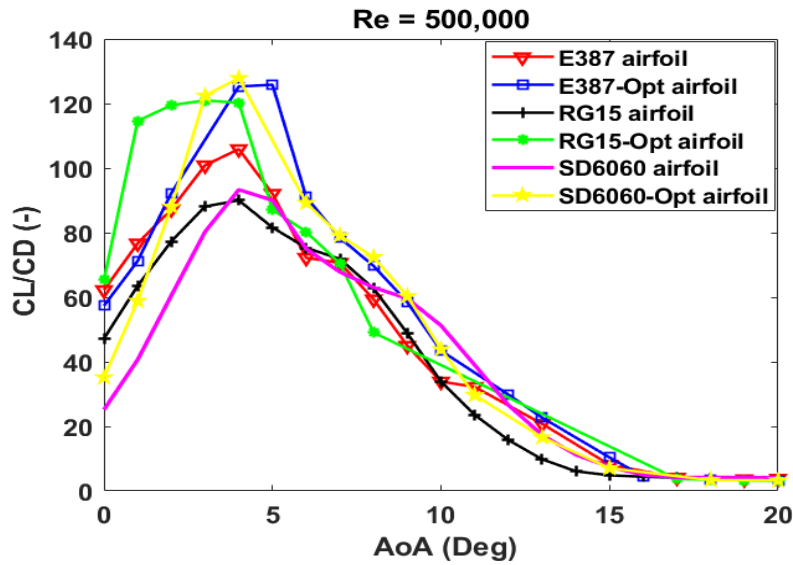
Fig. 13. Comparison of base and modified airfoils' CL/CD performances at Re of 500,000.

Fig. 14 shows the CL/CD efficiency of different airfoils, including the reference and altered ones, at a Re of 600,000. The E387-Opt airfoil performs better than the base and other modified airfoils when it comes to CL/CD investigations, especially at AoA between 2° and 13°. At an AoA of 4°, the E387-Opt airfoil recorded the highest maximum CL/CD of 135.16, while the maximum CL/CD of the E387 airfoil was 109.20 at the same AoA. Additionally, the shape modification of the RG15 airfoil improved the maximum CL/CD from 92.92 at an AoA of 4° to 127.11 at an AoA of 3°, and the SD6060-Opt airfoil increased the maximum CL/CD from 97.70 at an AoA of 4° (base SD6060 airfoil) to 134.99 at an AoA of 4°.
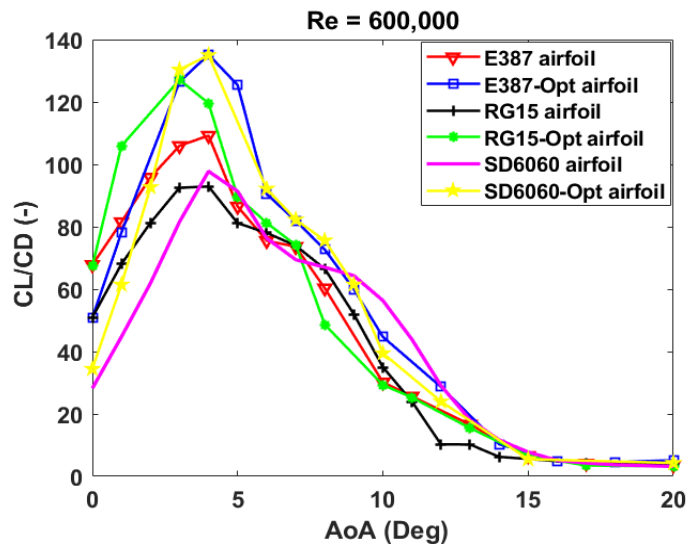

Fig. 14. Comparison of base and modified airfoils' CL/CD performances at Re of 600,000.

According to Fig. 15, we can see the CL/CD performance of six airfoils at a Re of 700,000. The E387-Opt airfoil shows the best CL/CD performance among all the airfoils, especially for angles of attack (AoA) from 2° to 20°. Its highest maximum CL/CD of 143.17 was recorded at an AoA of 4°. In comparison, the E387 airfoil's maximum was 112.60 at an AoA of 3°, which is significantly less. The RG15-Opt airfoil slightly increased the maximum CL/CD from 95.44 for the RG15 base airfoil to 132.23 without changing the AoA of 3°. On the other hand, the SD6060-Opt airfoil improved the maximum CL/CD from 98.33 to 140.07 without changing the AoA of 4°, compared to the values for the SD6060 airfoil.
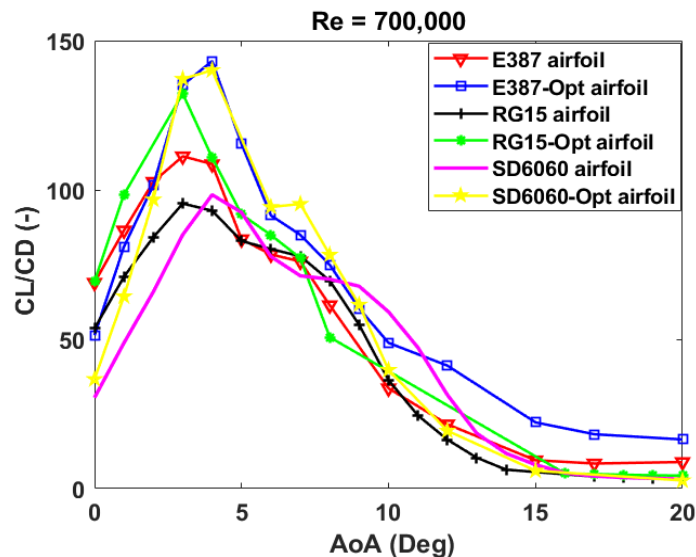
Fig. 15. Comparison of the CL/CD performances of base and modified airfoils at Re of 700,000.

Fig. 16 shows the CL/CD performance of the airfoils at a Re of 800,000. The E387-Opt airfoil performs better than the other airfoils, especially for AoA from 4° to 14°, with its highest maximum CL/CD of 150.06 recorded at an AoA of 4°, improving on the maximum CL/CD of the E387 airfoil, 113.30 at an AoA of 3°. After modifying the shape of the RG15 airfoil, the maximum CL/CD increased from 96.20 at an AoA of 3° to 136.20 at an AoA of 3°, while the SD6060-Opt airfoil increased the maximum CL/CD of the base SD6060 airfoil from 97.60 at an AoA of 4° to 145.42 at an AoA of 4°.
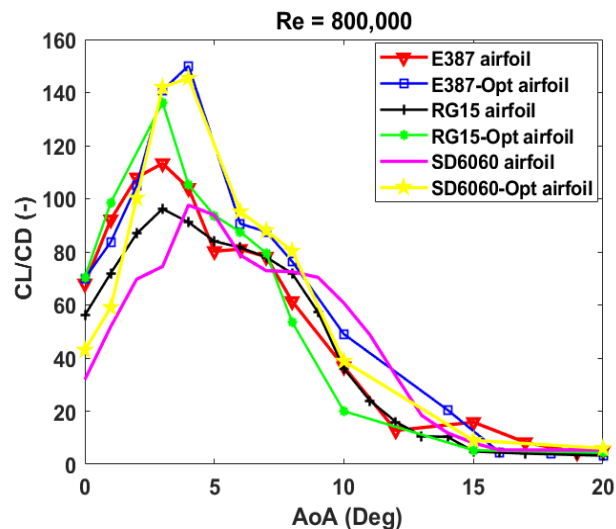

Fig. 16. Comparison of the CL/CD performances of base and modified airfoils at Re of 800,000.

The graph in Fig. 17 shows the CL/CD performance of six different airfoils, all tested at a Re of 900,000. The E387-Opt airfoil had the best performance in terms of CL/CD ratio, especially for angles of attack between 3° and 14°. At an angle of attack of 4°, this airfoil had the highest maximum CL/CD of 155.13. The modified version of the E387 airfoil also had a significant increase in maximum CL/CD, from 116.70 at an AoA of 3° to 155.13 at an AoA of 4°. The shape of the RG15 airfoil was altered to achieve similar results, with maximum CL/CD improving from 96.43 at an AoA of 3° to 140.38 at an AoA of 3°. Similarly, the modified airfoil SD6060 saw an increase in maximum CL/CD from 97.30 at an AoA of 4° to 148.97 at an AoA of 4°.
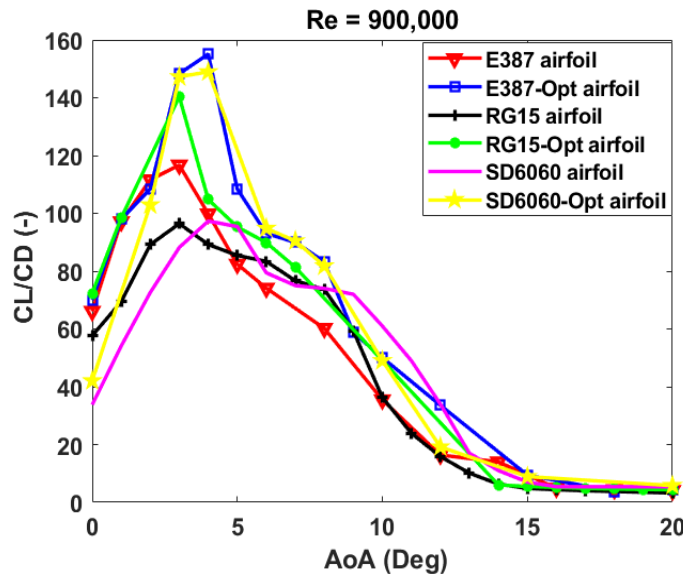
Fig. 17. Comparison of base and modified airfoils' CL/CD performances at Re of 900,000.

Fig. 18 illustrates the CL/CD performance of the studied airfoils at a Re of 1,000,000. As with the other evaluations, the E387-Opt airfoil performs better than the other airfoils, particularly for AoA from 3° to 20°, with the highest CL/CD of 161.17 at an AoA of 4°. The maximum CL/CD of the E387 airfoil has enhanced from 116.40 at an AoA of 3° to 161.17 at an AoA of 4° with the E387-Opt shape. Modifying the shape of the RG15 airfoil allowed its maximum CL/CD to be improved from 94.85 at an AoA of 3° to 143.48 at an AoA of 3° for the RG15-Opt. Finally, modifying the SD6060 airfoil increased the maximum CL/CD from 97.25 at an AoA of 4° to 152.60 at an AoA of 4° for the SD6060-Opt airfoil.
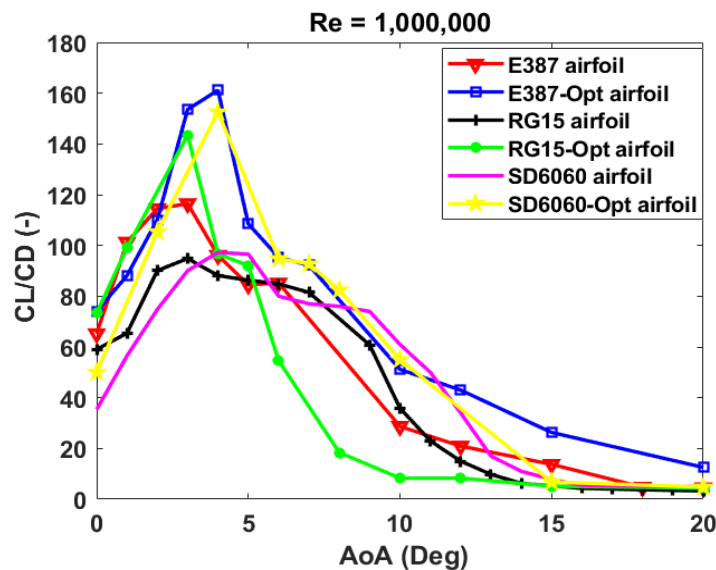

Fig. 18. Comparison of base and modified airfoils' CL/CD performances at Re of 1,000,000.

3.2.2. Investigating the peak CL/CD of the modified airfoils
Figs. 19 to 21 represent the maximum CL/CD for the E387-Opt, RG-15-Opt, and SD6060-Opt airfoils. As shown in Fig. 19, the E387-Opt airfoil at a Re of 1,000,000 performs better in terms of maximum CL/CD value than the other Re. The highest maximum CL/CD occurred at Re of 1,000,000, 161.17 at an AoA of 4°. The lowest maximum CL/CD occurred at Re of 500,000, 125.82 at an AoA of 5°. The maximum CL/CD values of 155.13, 150.06, 143.17, and 135.16 were recorded at Re of 900,000, 800,000, 700,000, and 600,000, respectively.
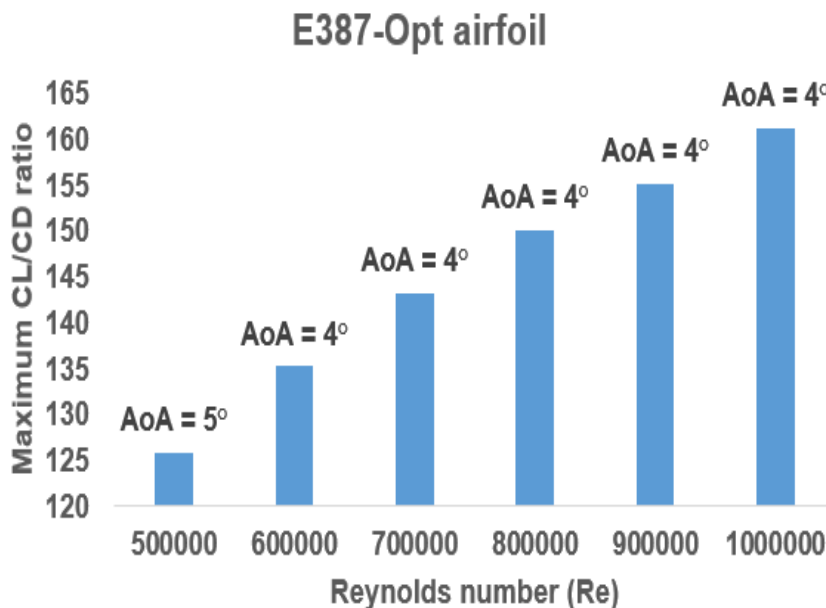
E387-Opt airfoil

Fig. 19. The maximum CL/CD variation with the AoA of the E387-Opt airfoil.

As shown in Fig. 20, the RG15-Opt airfoil at a Re of 1,000,000 performs better in terms of maximum CL/CD value than the other Re. The highest maximum CL/CD occurred at Re of 1,000,000, 143.48 at an AoA of 3º. The lowest maximum CL/CD occurred at Re of 500,000, 120.95 at an AoA of 3º. The maximum CL/CD values of 140.38, 136.20, 132.23, and 127.11 were recorded at Re of 900,000, 800,000, 700,000, and 600,000, respectively.
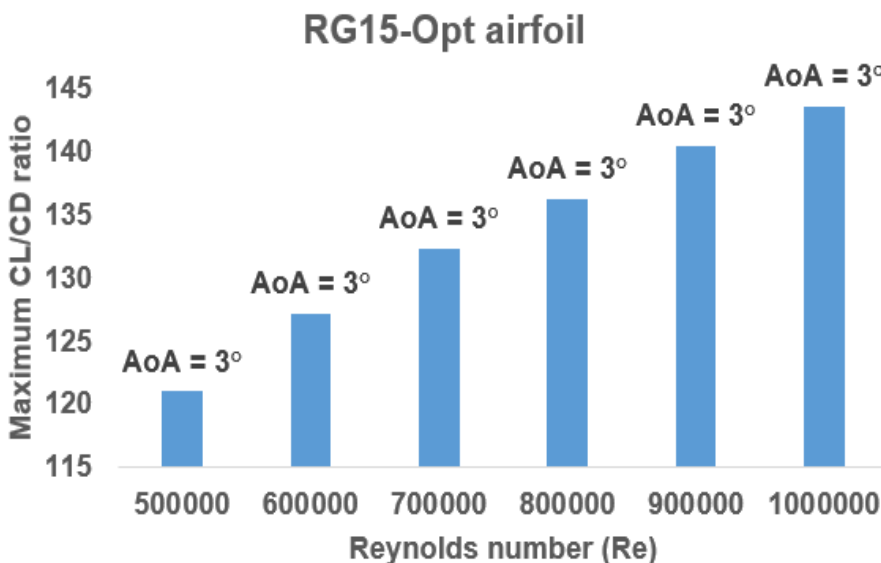
RG15-Opt airfoil

Fig. 20. The maximum CL/CD variation with the AoA of the RG15-Opt airfoil.

As shown in Fig. 21, the SD6060-Opt airfoil at a Re of 1,000,000 performs better in terms of maximum CL/CD value than the other Re. The highest maximum CL/CD occurred at Re of 1,000,000, 152.60 at an AoA of 4º. The lowest maximum CL/CD occurred at Re of 500,000, 127.89 at an AoA of 4º. The maximum CL/CD values of 148.97, 145.42, 140.07, and 134.99 were recorded at Re of 900,000, 800,000, 700,000, and 600,000, respectively.
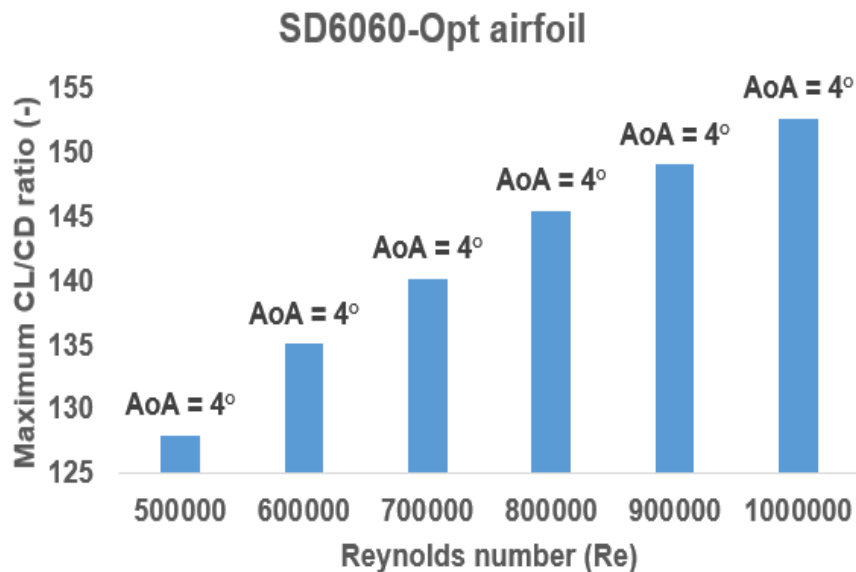
Fig. 21. The maximum CL/CD variation with the AoA of the SD6060-Opt airfoil.

The evaluations have demonstrated that the E387-Opt, RG15-Opt, and SD6060-Opt airfoils have better performance than the base airfoils. The modified versions have consistently performed better across all the tested Reynolds numbers. Additionally, the results obtained by Islam (2008) and Uddin et al. (2023) have shown that the effectiveness of an airfoil can be determined by analyzing the CL/CD.

4. Conclusion

The study evaluated the aerodynamic efficiency of the modified and unmodified versions of the E387-Opt, RG15-Opt, and SD6060-Opt airfoils for their maximum CL/CD purposes using XFOIL software at six intervals of Re ranging from 500,000 to 1,000,000. As the Re increased in this range, the maximum CL/CD decreased. The results of the study are summarized below:
- The modified airfoils' ideal % t/c had higher maximum CL/CD values than those of the reference airfoils for Re, ranging from 500,000 to 1,000,000. The E387 airfoil had a maximum CL/CD increase of 0.50% to 1.30%, the RG15 airfoil increased by 0.58% to 1%, and the SD6060 airfoil increased by 0.40% to 1%, respectively.
- The modified E387, RG15, and SD6060 airfoils showed that the highest maximum CL/CD occurred in the t/c% of 0.64%, 0.74%, and 0.47%, respectively.
- The E387-Opt airfoil increased the maximum CL/CD by 18.92% at a Re of 500,000, 23.77%

at a Re of 600,000, 27.14% at a Re of 700,000, 32.44% at a Re of 800,000, 32.93% at a Re of 900,000, and 38.46% at a Re of 1,000,000.
- The RG15-Opt airfoil increased the maximum CL/CD by 34.38% at a Re of 500,000, 36.75% at a Re of 600,000, 38.54% at a Re of 700,000, 41.58% at a Re of 800,000, 45.57% at a Re of 900,000, and 51.30% at a Re of 1,000,000.
- The SD6060-Opt airfoil increased the maximum CL/CD by 37.07% at a Re of 500,000, 38.16% at a Re of 600,000, 42.44% at a Re of 700,000, 48.99% at a Re of 800,000, 53.10% at a Re of 900,000, and 56.91% at a Re of 1,000,000.
These results suggest that modifying SWT airfoils using the ideal %t/c significantly increased their performance regarding the maximum CL/CD. Future work will involve conducting multiple experimental tests across a range of Re between 500,000 to 1,000,000 for modified and base airfoils. In particular, 3-bladed horizontal axis wind turbines developed in the context of this work will next be subjected to extensive Computational Fluid Dynamics (CFD) Simulation, Particle Image Velocimetry (PIV) flow visualization, and wind tunnel testing by the Solar Turbine Arta Energy Company.

Nomenclature

Roman symbol

c	Chord of length (m)
% c	Percentage of chord (-)
C_D	Drag Coefficient (-)
C_L	Lift Coefficient (-)
C_L/C_D	Lift-to-drag ratio (-)
D	Drag force (N)
l	Airfoil span (m)
L	Lift force (N)
Re	Reynolds number (-)
t/c%	Thickness-to-camber ratio percentages (-)

Acronyms

AoA	Angle of Attack
CFD	Computational Fluid Dynamics
PIV	Particle Image Velocimetry
SWT	Small Wind Turbine

Greek Symbol

ρ	Airflow density (Kg/m^3)
μ	Dynamic viscosity ($Kg\ m^{-1}s^{-1}$)
υ	Kinematic viscosity (m^2s^{-1})

References

Anastasiia, N., 2022. Design of an airfoil by mathematical modeling using database. *Journal of Airline Operations and Aviation Management*: 1, 19-26.

Bhavsar, H., Roy, S. & Niyas, H., 2023. Multi-element airfoil configuration for HAWT: A novel slot design for improved aerodynamic performance. *Materials Today: Proceedings*: 72, 386-393. https://doi.org/10.1016/j.matpr.2022.08.110

Chen, D., Xu, R., Yuan, Z., Pan, G. & Marzocca, P., 2023. The effect of vortex induced vibrating cylinders on airfoil aerodynamics. *Applied Mathematical Modelling*: 115, 868-885. https://doi.org/10.1016/j.apm.2022.12.001

Drela, M., 1989. XFOIL: An analysis and design system for low Reynolds number airfoils. In Low Reynolds Number Aerodynamics: Proceedings of the Conference Notre Dame, Indiana, USA, 5–7 June. Berlin, *Heidelberg: Springer Berlin Heidelberg*: 1-12. https://doi.org/10.1007/978-3-642-84010-4_1

Drela, M. & Youngren, H., 2001. XFOIL 6.94 User Guide, MIT Aero & Astro.

Flynn, Z. & Goza, A., 2023. Flow physics of a passive flap on a dynamically pitched airfoil. *In AIAA SCITECH 2023 Forum* (p. 1791). https://doi.org/10.2514/6.2023-1791

Islam, M., 2008. Analysis of fixed-pitch straight-bladed VAWT with asymmetric airfoils.

Jaffar, H., Al-Sadawi, L., Khudhair, A. & Biedermann, T., 2023. Aerodynamics improvement of DU97-W-300 wind turbine flat-back airfoil using slot-induced air jet. *International Journal of Thermofluids*: 17, 100267. https://doi.org/10.1016/j.ijft.2022.100267

Kasmaiee, S., Tadjfar, M. & Kasmaiee, S., 2023. Optimization of Blowing Jet Performance on Wind Turbine Airfoil Under Dynamic Stall Conditions Using Active Machine Learning and Computational Intelligence. *Arabian Journal for Science and Engineering*: 1-25. https://doi.org/10.1007/s13369-023-07892-9

Lei, J., Zhang, J. & Niu, J., 2020. Effect of active oscillation of local surface on the performance of low Reynolds number airfoil. *Aerospace Science and Technology*: 99, 105774. https://doi.org/10.1016/j.ast.2020.105774

Leloudas, S.N., Eskantar, A.I., Lygidakis, G.N. & Nikolos, I.K., 2020. Low Reynolds airfoil family for small horizontal axis wind turbines based on RG15 airfoil. *SN Applied Sciences*: 2. https://doi.org/10.1007/s42452-020-2161-1

Manwell, F., Jon, G., Gowan, M. & Rogers, A., 2010. Wind energy explained: theory, design and application, John Wiley & Sons.

Mohamed, O.S., Ibrahim, A.A., Etman, A.K., Abdelfatah, A.A. & Elbaz, A.M., 2020. Numerical investigation of Darrieus wind turbine with slotted airfoil blades. *Energy Conversion and Management*: X, 5, 100026. https://doi.org/10.1016/j.ecmx.2019.100026

Morgado, J., Vizinho, R., Silvestre, M.A.R. & Páscoa, J.C., 2016. XFOIL vs CFD performance predictions for high lift low Reynolds number airfoils. *Aerosp Sci Technol*: 52, 207-214. https://doi.org/10.1016/j.ast.2016.02.031

Nichols, R. & Buning, P., 2021. User's Manual for OVERFLOW 2.3, NASA Langley Research Center. February.

Özden, M., Genç, M.S. & Koca, K., 2023. Passive Flow Control Application Using Single and Double Vortex Generator on S809 Wind Turbine Airfoil. *Energies*: 16(14), 5339. https://doi.org/10.3390/en16145339

Ramanujam, G., Özdemir, H. & Hoeijmakers, H.W.M., 2016. Improving airfoil drag prediction. Journal of Aircraft: 53, 1844-1852. https://doi.org/10.2514/1.C033788

Seifi, H., Kouravand, S. & Seifi Davary, M., 2023. Numerical and experimental study of NACA airfoil in low Reynolds numbers for use of Darriues vertical axis micro-wind turbine. *Journal of Renewable and New Energy*: 10(2), 149-163. https://doi.org/10.52547/JRENEW.10.2.149

Seifi, H., Kouravand, S., Davary, M.S. & Mohammadzadeh, S., 2023. Numerical and

Experimental study of the effect of increasing aspect ratio of self-starting force to vertical axis wind turbine. *Journal of Renewable and New Energy*: 10(1), 1-14. https://doi.org/10.52547/JRENEW.10.1.1

Seifi Davari, H., Kouravand, S., Seify Davari, M. & Kamalnejad, Z., 2023. Numerical investigation and aerodynamic simulation of Darrieus H-rotor wind turbine at low Reynolds numbers, *Energy Sources, Part A: Recovery, Utilization, and Environmental Effects*: 45(3), 6813-6833. https://doi.org/10.1080/15567036.2023.2213670

Shi, X., Xu, S., Ding, L. & Huang, D., 2019. Passive flow control of a stalled airfoil using an oscillating micro-cylinder. *Computers & Fluids*: 178, 152-165. https://doi.org/10.1016/j.compfluid.2018.08.012

Tirandaz, M.R. & Rezaeiha, A., 2021. Effect of airfoil shape on power performance of vertical axis wind turbines in dynamic stall: Symmetric Airfoils. *Renewable Energy*: 173, 422-441. https://doi.org/10.1016/j.renene.2021.03.142

Uddin, S.N., Haque, M.R., Haque, M.M., Alam, M.F. & Hamja, A., 2023, Numerical Investigation of the Enhancement of the Aerodynamic Performance for Newly Modified Blended Airfoils Utilizing S809, S829, and NACA 2412 Baseline Shapes. *Arabian Journal for Science and Engineering*: 1-16. https://doi.org/10.1007/s13369-023-08180-2

Wani, I.N., Bhaskar, B., Raghuwanshi, S.S., Kushwah, N., Agrawal, Y., Kumar, A., Pandey, A. & Ayachit, B., 2023. Design & analysis of NACA 0012 airfoil with circular dent of 30 mm depth on upper surface. *Materials Today: Proceedings*. https://doi.org/10.1016/j.matpr.2023.05.013

Wu, L., Liu, X., Liu, Y. & Xi, G., 2022. Using the combined flow control accessory to the aerodynamic performance enhancement of bio-inspired seagull airfoils. *Journal of Renewable and Sustainable Energy*: 14(2). https://doi.org/10.1063/5.0079060

Ye, X., Hu, J., Zheng, N. & Li, C., 2023. Numerical study on aerodynamic performance and noise of wind turbine airfoils with serrated gurney flap. *Energy*: 262, 125574. https://doi.org/10.1016/j.energy.2022.125574

Zhang, Y.N., Cao, H.J. & Zhang, M.M., 2021. Investigation of leading-edge protuberances for the performance improvement of thick wind turbine airfoil1. *Journal of Wind Engineering and Industrial Aerodynamics*: 217, 104736. https://doi.org/10.1016/j.jweia.2021.104736.